

Earthquakes Triggered by Silent Slip Events on Kīlauea Volcano, Hawai‘i

Paul Segall, Emily K. Desmarais, David Shelly

Department of Geophysics
Stanford University

Asta Miklius, USGS, Hawai‘i Volcano Observatory

Peter Cervelli, USGS, Alaska Volcano Observatory

April 27, 2006

Slow slip events, or silent earthquakes, have been recently discovered in a number of subduction zones including the Nankai trough, Japan^{1;2;3}, Cascadia^{4;5}, and Guerrero, Mexico⁶. Depths of these events have been difficult to determine from surface deformation measurements. While it is assumed that they are located along the plate megathrust, this has not been proven. Slow slip in some subduction zones is associated with non-volcanic tremor^{7;8}, however tremor is difficult to locate and may be distributed over a broad depth range⁹. Except for some events on the San Andreas fault¹⁰, slow slip events have not yet been associated with high frequency earthquakes, which are easily located. We report here on swarms of high-frequency earthquakes that accompany otherwise silent slips on Kīlauea volcano. For the most energetic, January 2005 event, the slow slip began before the increase in seismicity. The temporal evolution of earthquakes is well explained by increased stressing caused by slow slip, implying the quakes are triggered. The earthquakes, located at depths of 7-8 km, constrain the slow slip to be at comparable depths, since they must fall in zones of positive Coulomb stress change. Triggered earthquakes accompanying slow slip events elsewhere might go undetected if background seismicity rates are low. Detection of such events would help constrain the depth of slow slip, and could lead to a method for quantifying the increased hazard during slow slip events, since triggered events have the potential to grow into destructive earthquakes.

A silent earthquake beneath the south flank of Kīlauea on 10-11 November 2000 displaced GPS stations as much as 1.5 cm over \sim 36 hours¹¹. The depth of the subhorizontal fault was not well constrained, but inversions favored depths of 4-5 km, considerably shallower than the decollement thought to occur at the base of the volcano. We now recognize similar events on 20-21 September 1998, 7-8 July 2003, and 25-26 January 2005 (additional events have subsequently been reported¹²). All four events have similar durations and displacement patterns (Figure 1 and 2). Inversions assuming uniform slip dislocations place the four sources in virtually the same location (Figure 1). While the November 2000 slow slip was preceded by extreme rainfall¹¹, the other events were not.

All four slow slip events were associated with heightened levels of microseismicity (Figure 2). The cumulative magnitude of the microearthquakes is far too small to explain the observed

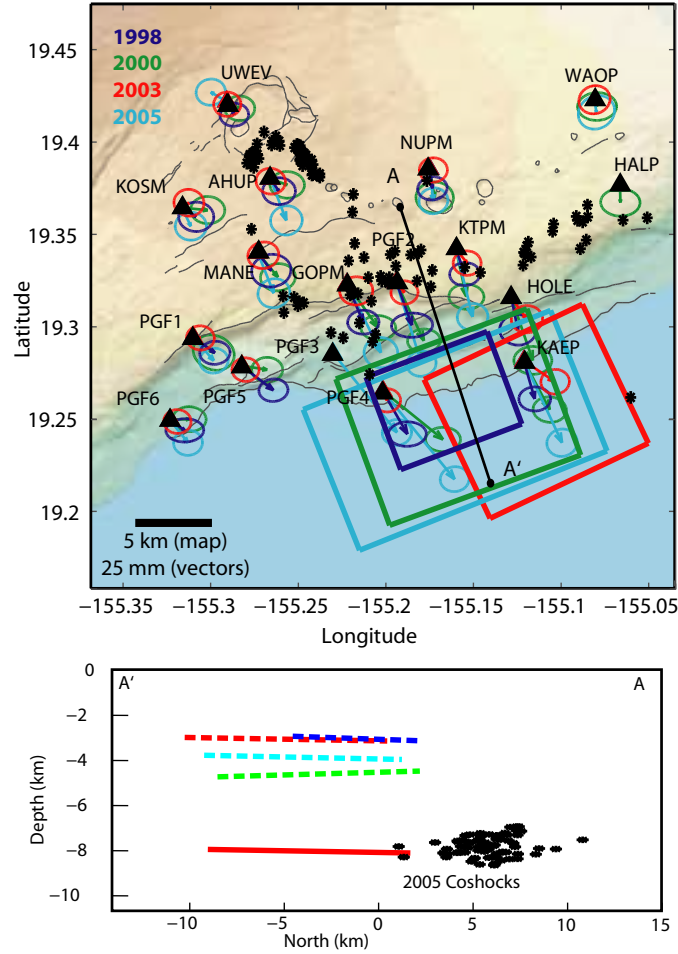


Figure 1: Displacements and inferred slip zones for four silent slip events. Displacements are determined as the difference between the mean position before and after the event. Rectangles show surface projections of best fitting dislocations found by non-linear optimization using a simulated annealing procedure¹³. Circles indicate relocated earthquakes accompanying the 2005 slip event. In cross section dashed lines represent GPS inversion results. Solid line indicates 2005 event with depth constrained by seismicity.

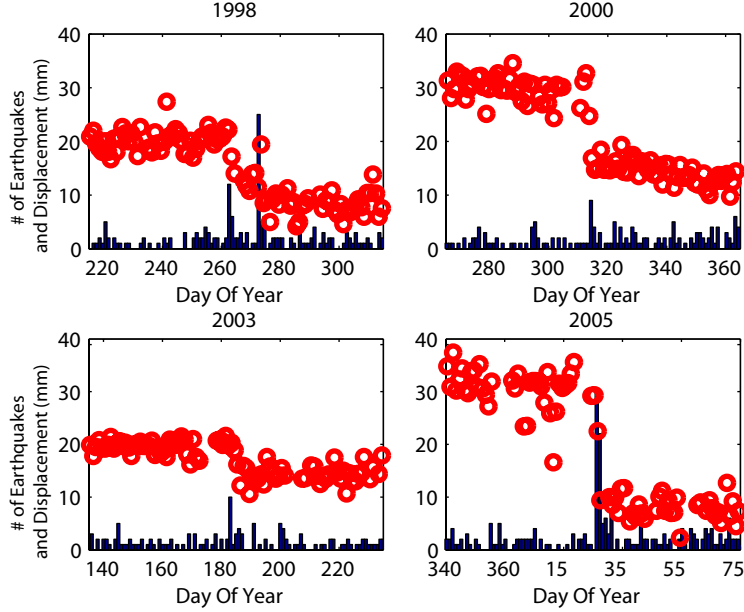


Figure 2: North displacement of GPS station KAPE (open circles) and number of south flank earthquakes per day (histogram). Note that the seismicity rate increases during periods of rapid displacement.

displacements. For example, the cumulative moment of the 2005 earthquake swarm is $\sim 1.8 \times 10^{14}$ N-m, far less than that of the slow slip, 6.8×10^{17} N-m. The microearthquakes, which are concentrated adjacent to the landward edge of the dislocation (Figure 1), are thus not the source of the deformation.

The association of high frequency earthquakes with slow slip could be explained by either 1) the earthquakes unpinning the fault, allowing slow slip to occur, or 2) the slow slip stressing the adjacent fault, thereby increasing the seismicity rate. To constrain the onset and duration of fault slip relative to the microearthquakes, we invert the GPS observables during the 2005 slow event directly for fault slip as a function of time¹¹. The slow slip started early on January 26, 2005, well before the dramatic increase in seismicity, and continued for approximately two days (Figure 3), supporting the second interpretation. The triggered earthquakes are thus properly thought of as “co-shocks” and aftershocks of the otherwise silent earthquakes.

Dieterich’s seismicity rate theory¹⁴ is used to quantitatively relate the slip and seismicity. The seismicity rate R is related to the background seismicity rate r and a state variable γ , as

$$R = \frac{dN}{dt} = \frac{r}{\gamma \dot{\tau}_r} \quad (1)$$

where N is the number of events, and $\dot{\tau}_r$ is the background stressing rate. The seismicity state variable evolves according to

$$d\gamma = \frac{1}{a\sigma} [dt - \gamma d\tau + \gamma(\tau/\sigma - \alpha)d\sigma] \quad (2)$$

where a and α are constitutive constants, and τ and σ are the shear and effective normal stress, respectively. Because normal stress variations may be largely balanced by undrained changes in pore pressure, we assume $d\sigma = 0$; in fact the stress variations are understood to be changes in the Coulomb stress. Dieterich¹⁴ showed that the seismicity rate following a step change in

shear stress $\Delta\tau$ followed by a return to the background stressing rate $\dot{\tau}_r$ yields the modified Omori law with aftershock duration given by $t_a = a\sigma/\dot{\tau}_r$.

To model the triggered seismicity, we approximate the slip history with a ramp function (Figure 3b). Prior to the onset of accelerated slip, $t < t_0$, the background stressing rate is $\dot{\tau}_r$. During the event $t_0 < t < t_1$ the stressing rate increases to $\dot{\tau}$; for $t > t_1$ the stressing rate returns to background. For this stress history the predicted seismicity rate is found from (1) and (2) (Methods). To compare with observations we compute the cumulative number of earthquakes, $N(t)$ determined by integrating $R(t)$

$$N(t) = \begin{cases} rt_a \ln \left[\frac{\dot{\tau}_r}{\dot{\tau}} \left(\exp \left(\frac{\dot{\tau}(t-t_0)}{a\sigma} \right) - 1 \right) + 1 \right] & t_0 < t < t_1 \\ rt_a \ln \left[\frac{\exp \left(\frac{t-t_1}{t_a} \right) + C}{1+C} \right] & t > t_1 \end{cases} \quad (3)$$

where

$$C = \left[\left(1 - \frac{\dot{\tau}_r}{\dot{\tau}} \right) \exp \left(-\frac{\dot{\tau}(t_1 - t_0)}{a\sigma} \right) + \frac{\dot{\tau}_r}{\dot{\tau}} - 1 \right]. \quad (4)$$

$N(t)$ depends on five parameters: 1) the background rate r , 2) the aftershock decay time, t_a ; 3) the ratio of the event to background stressing rate, $\dot{\tau}/\dot{\tau}_r$, 4) the onset t_0 and 5) duration $t_1 - t_0$, of the slip event. Note that $\dot{\tau}/a\sigma = \dot{\tau}/\dot{\tau}_r t_a$.

The background rate r of ~ 1.33 events/day is estimated from the earthquake catalog before and well after the slow slip event. The onset time (UTC midnight on January 26) and duration (2.2 days) of the slow event are determined from the GPS data (Figure 3b). t_a of 10 to 20 days is found from the decay of aftershocks following the September 3, 1997, M 5.5 south flank earthquake. The only parameter not determined *a priori* is the ratio of stressing rates $\dot{\tau}/\dot{\tau}_r$.

We fit the cumulative number of earthquakes to equation (3) with $t_a = 10$. The best fit, obtained for an increase in stressing rate of a factor of 33, provides satisfactory agreement with the earthquake data (Figure 3), especially considering the single adjustable parameter. A better fit is obtained by reducing t_a to 7 days. Whether this indicates temporal or spatial variation in t_a (the 1997 earthquake was roughly 20 km from the swarm earthquakes) is unknown.

The spatial association of the silent slip and its co-shocks is clear in map view, however the depth of the slow slip event is difficult to constrain solely on the basis of the GPS observations. While the catalog earthquake depths are scattered over a broad range, relocations of south flank earthquakes illuminate a sub-horizontal plane^{15,16}. Hansen et al.¹⁷ utilized a temporary deployment of 29 three component seismometers along with the HVO permanent network to jointly locate earthquakes and determine the 3D seismic velocity structure. They found that earthquakes occurring on the central south flank from November 1999 to June 2000, lie on a nearly horizontal surface at a depth of 7 to 9 km.

The Hansen et al.¹⁷ hypocenters can be used to improve the locations of the swarm events accompanying slow slips. We focus on the most energetic January 2005 swarm. Based on catalog locations, we believe quakes during the other slow events are located at comparable depths. A “double difference”¹⁸ relocation of the January 2005 swarm events relative to the 1999-2000 events (see Methods) demonstrates that the swarm events were located at the same depth as the background seismicity, 7 to 9 km (Figure 1).

The depth of the swarm earthquakes, and the likelihood they were triggered by the slow slip, constrains the depth of the slow slip. Specifically, slow slip must have occurred at depths for which the induced stresses favor slip in the swarm. If the slow slip is too shallow the earthquakes locate in a stress shadow and are thus inconsistent with triggering. Varying the depth of the best fitting dislocation maps the depth range consistent with the triggered earthquakes (Figure 4).

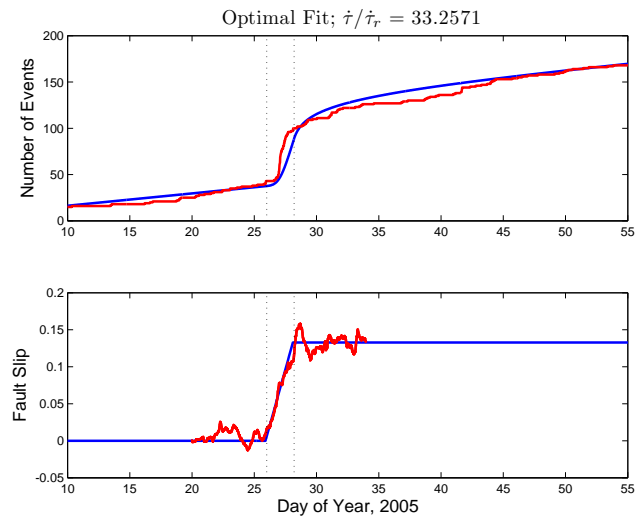


Figure 3: Fit of seismicity data to that predicted from stressing due to the silent slip event. (a) Cumulative number of earthquakes as a function of the day of the year, 2005. Observed earthquake count in hourly bins (red), compared to that predicted by equation (3) for the slow slip event (blue). Vertical dotted lines mark the beginning and end of the slow slip event as determined from the GPS data below. (b) Inverted slip history estimated directly from the GPS phase data (red), using a Kalman filter procedure described in Methods. Fault slip is allowed to vary as a random walk in time¹¹, with scale parameter $\sigma_s = 0.015\text{mm}/\text{yr}^{1/2}$. Ramp function illustrates the stress history used to derive the predicted seismicity rate (blue).

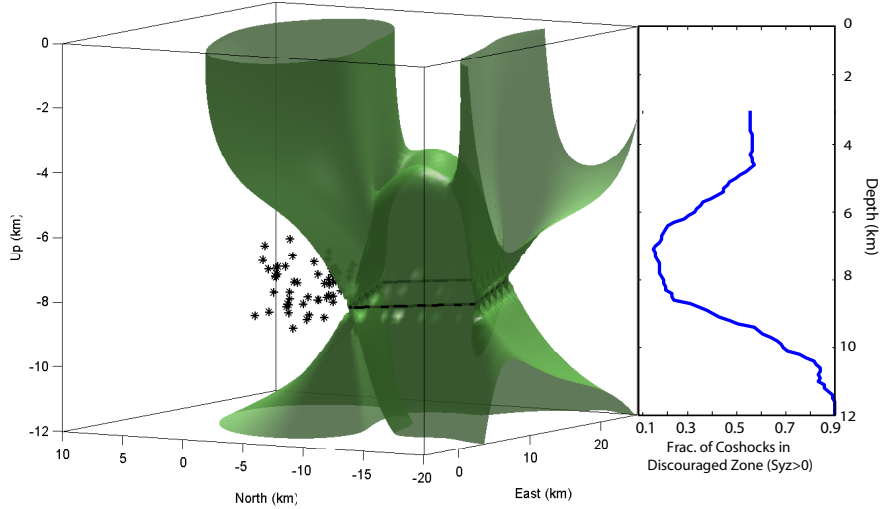


Figure 4: (left) January 2005 earthquakes and isosurface of constant Coulomb stress change on horizontal surfaces. Outside the green surface the stress change encourages slip. For a dislocation surface at 4-5 km depth, a majority of the earthquakes fall within the zone of negative Coulomb stress change. (right) Fraction of earthquakes discouraged by slow slip as a function of the depth of the slow slip event. Minimum at a depth of 7-8 km indicates the preferred depth of the slow slip zone.

The best fit occurs when the slip event is at the same depth as the earthquakes, 7-8 km. At this depth the shear stress concentration at the edge of the dislocation is focussed on the earthquake swarm. The silent slip event and its co-shocks are thus most likely coplanar and located at a depth of 7 to 8 km.

Is the depth of the silent slip event inferred from the earthquakes consistent with the geodetic observations? The best fitting dislocation constrained to depths between 7.5 and 8.5 km (Figure 5) is in fact consistent with the data at the few mm level. Depth varying elastic properties and non-planar topography favor deeper sources relative to uniform half-space models, although the effect is relatively minor.

Kīlauea suffered a $M_w 7.7$ earthquake and tsunami in 1975¹⁹. Despite the fact that both geodetic data²⁰ and the tsunami source²¹ require slip offshore, the aftershocks were restricted to a narrow strip between the rift zones and the coastline. Indeed, south flank earthquakes rarely occur offshore despite the fact that the geodetic data require extensive slip there^{22,23}. These observations indicate a transition from stick slip behavior between the rift zone and the coast to stable sliding offshore. Slow slip events seem to occur in the transition between these two domains. Modeling studies indicate that transient slip events occur in transitions from velocity weakening to velocity strengthening friction²⁴, or where velocity weakening patches in an otherwise creeping fault are near the critical nucleation dimension²⁵. On Kīlauea the transition in frictional behavior might result from temperature and pressure variations with distance from the rift zone²⁶.

Our results have implications for silent slip events in subduction zones. (A slow earthquake on the San Andreas Fault¹⁰ appears to have been in part triggered by a sequence of M 3+ earthquakes, which initiated two hours before detectable strain changes, and is thus very different from the Kīlauea slow events). Microseismicity rates on Kīlauea are much higher than in

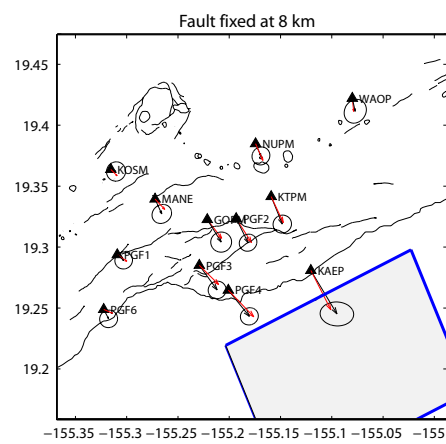


Figure 5: Observed (black with 95% confidence ellipses) and predicted (red) displacements during the January 2005 silent slip event with dislocation constrained to depths of 7.5 to 8.5 km.

some subduction zones. A rate increase of a factor of 35 is dramatic on Kīlauea, but might go unnoticed in subduction zones with few earthquakes located on the plate interface. Given our findings a concerted effort should be made to search for very small earthquakes accompanying slow slip events elsewhere.

Slow slip events in subduction zones appear to be located down-dip of the locked zone so that transient slip acts to stress the seismogenic fault. If small events are triggered, as we observe on Kīlauea, then the potential exists for one of these to grow into a destructive earthquake. A M_w 6.7 thrust earthquake coincided with the end of the 2002 slow slip event in Guerrero, Mexico²⁴. It is possible to quantify the increased hazard associated with slow slip events by the increase in seismicity rate, which depends on the duration of the slow slip relative to t_a and the increase in stressing rate $\dot{\tau}/\dot{\tau}_r$. The peak seismicity rate $1/(C + 1)$ occurs at the end of the slow slip event t_1 (See Methods). Of course, the nucleation of an earthquake does not determine its ultimate size. The longer the plate boundary remains locked, however, the higher the ambient stresses become, and the more likely it is that a triggered event can grow into a major earthquake. It is possible that as the stress increases the size of co-shocks triggered during slow events will increase, making them more easily detected.

Acknowledgments. We gratefully acknowledge Cliff Thurber for providing seismic data from the Univ. of Wisconsin 1999/2000 experiment, Paul Okubo for help with H.V.O. seismic data, and the University of Hawaii for exchange of seismic data.

References

- [1] H. Hirose, K. Hirahara, F. Kimata, N. Fujii, and S. Miyazaki. A slow thrust slip event following the two 1996 Hyuganada earthquakes beneath the Bungo Channel, southwest Japan. *Geophysical Research Letters*, 26(21):3237 – 40, 1999 1999.
- [2] S. Ozawa, M. Murakami, M. Kaidzu, T. Tada, T. Sagiya, Y. Hatanaka, H. Yarai, and T. Nishimura. Detection and monitoring of ongoing aseismic slip in the Tokai region, central Japan. *Science*, 298:1009–1012, 2002.
- [3] S. Miyazaki, J. McGuire, and P. Segall. A transient subduction zone slip episode in southwest Japan observed by the nationwide GPS array. *J. Geophys. Res.*, 108(B2):2087–2087, Feb 2003.
- [4] H. Dragert, K. L. Wang, and T. S. James. A silent slip event on the deeper Cascadia subduction interface. *Science*, 292(5521):1525 – 8, May 2001.
- [5] M. M. Miller, T. Melbourne, D. J. Johnson, and W. Q. Sumner. Periodic slow earthquakes from the Cascadia subduction zone. *Science*, 295(5564):2423 – 2423, MAR 2002.
- [6] V. Kostoglodov, S. K. Singh, J. A. Santiago, S. I. Franco, K. M. Larson, A. R. Lowry, and R. Bilham. A large silent earthquake in the Guerrero seismic gap, Mexico. *Geophysical Research Letters*, 30(15):1807 –, Aug 2003.
- [7] G. Rogers and H. Dragert. Episodic tremor and slip on the Cascadia subduction zone: The chatter of silent slip. *Science*, 300(5627):1942 – 3, Jun 2003.
- [8] K. Obara, H. Hirose, F. Yamamizu, and K. Kasahara. Episodic slow slip events accompanied by non-volcanic tremors in southwest Japan subduction zone. *Geophysical Research Letters*, 31(23):L23602 –, Dec 2004.

- [9] H. Kao, Shao-Ju Shan, H. Dragert, G. Rogers, J. F. Cassidy, and K. Ramachandran. A wide depth distribution of seismic tremors along the northern Cascadia margin. *Nature*, 436,:841–844, Aug 2005.
- [10] A.T. Linde, M.T. Gladwin, M.J.S. Johnston, R.L. Gwyther, and R.G. Bilham. A slow earthquake sequence on the San Andreas fault. *Nature*, 383:65–68, Sep 1996.
- [11] P. Cervelli, P. Segall, K. Johnson, M. Lisowski, and A. Miklius. Sudden aseismic fault slip on the south flank of Kilauea volcano. *Nature*, 415(6875):1014 – 1018, Feb 2002.
- [12] B. Brooks, J. Foster, M. Bevis, L. Frazer, and M. Behn. Slow earthquakes on the flank of Kilauea volcano, hawaii. *Transactions AGU Fall Meeting Supplement*, 86(52):G53B–0879, 2005.
- [13] P. Cervelli, M.H. Murray, P. Segall, Y. Aoki, and T. Kato. Estimating source parameters from deformation data, with an application to the march 1997 earthquake swarm off the Izu Peninsula, Japan. *J. Geophys. Res.*, 106(6875):11,217–11,238, Feb 2001.
- [14] J. Dieterich. A constitutive law for rate of earthquake production and its application to earthquake clustering. *J. Geophys. Res.*, 99(B2):2601–2618, Feb 1994.
- [15] J. Got, J. Frechet, and F. Klein. Deep fault plane geometry inferred from multiplet relative relocation beneath the south flank of Kilauea. *Journal of Geophysical Research*, 99(B8):15375 – 86, Aug 1994.
- [16] J.-L. Got and P. Okubo. New insights into Kilauea’s volcano dynamics brought by large scale relative relocation of microearthquakes. *J. Geophys. Res.*, 108(B7):2337 – 2350, Jul 2003.
- [17] S. Hansen, C. Thurber, M. Mandernach, F. Haslinger, and C. Doran. Seismic Velocity and Attenuation Structure of the East Rift Zone and South Flank of Kilauea Volcano, Hawaii. *Bulletin of the Seismological Society of America*, 94(4):1430–1440, Aug 2004.
- [18] F. Waldhauser and W. L. Ellsworth. A Double-Difference Earthquake Location Algorithm: Method and Application to the Northern Hayward Fault, California. *Bulletin of the Seismological Society of America*, 90(6):1353–1368, Dec 2000.
- [19] M. Nettles and G. Ekstrom. Long-Period Source Characteristics of the 1975 Kalapana, Hawaii, Earthquake. *Bulletin of the Seismological Society of America*, 94(2):422–429, Apr 2004.
- [20] S.E. Owen and R. Burgmann. An increment of volcano collapse: Kinematics of the 1975 kalapana, hawaii, earthquake. *Journal of Volcanology and Geothermal Research*, in press:–, 2005.
- [21] Kuo-Fong Ma, H. Kanamori, and K. Satake. Mechanism of the 1975 Kalapana, Hawaii, earthquake inferred from tsunami data. *J. Geophys. Res.*, 104(B6):13153–13168, 1999.
- [22] P. Delaney, R. Denlinger, M. Lisowski, A. Miklius, P. Okubo, A. Okamura, and M. Sako. Volcanic spreading at Kilauea, 1976-1996. *J. Geophys. Res.*, 103(B8):18,003 – 18,023, Aug 1998.

- [23] S. Owen, P. Segall, M. Lisowski, A. Miklius, R. Denlinger, and M. Sako. Rapid deformation of Kilauea Volcano: Global positioning system measurements between 1990 and 1996. *J. Geophys. Res.*, 105(B8):18983 – 18998, Aug 2000.
- [24] Y. Liu and J. R. Rice. Aseismic slip transients emerge spontaneously in 3d rate and state modeling of subduction earthquake sequences. *Journal of Geophysical Research*, 110:B08307, doi:10.1029/2004JB003424, 2005.
- [25] N. Kato. Interaction of slip on asperities: Numerical simulation of seismic cycles on a two-dimensional planar fault with nonuniform frictional property. *Journal of Geophysical Research*, 109(B12306), Dec 2004.
- [26] P. Segall, P.F. Cervelli, and A. Miklius. Insights from deformation during the pu'u o'o eruption of Kilauea volcano. *EOS, American Geophysical Union, Fall Meeting 2002*, 2002.

Methods

Predicted Seismicity Rate.

At $t = 0$, γ takes the value $1/\dot{\tau}_r$. Ignoring changes in effective normal stress, for $0 < t < t_1$ the stressing rate is constant at $\dot{\tau}$, so that (2) reduces to

$$\frac{d\gamma}{dt} = \frac{1}{a\sigma}[1 - \gamma\dot{\tau}] \quad (5)$$

which has solution

$$\gamma = \left(\frac{1}{\dot{\tau}_r} - \frac{1}{\dot{\tau}} \right) \exp \left(-\frac{\dot{\tau}t}{a\sigma} \right) + \frac{1}{\dot{\tau}} \quad 0 < t < t_1 \quad (6)$$

given the initial condition $\gamma(t = 0) = 1/\dot{\tau}_r$. For $t > t_1$ the stressing rate is again constant, but at the background rate. The solution to (5) is thus of a similar form to (6), however the initial condition is now given by $\gamma_1 \equiv \gamma(t_1)$, equation (6) evaluated at t_1 . The result is

$$\gamma = \left(\gamma_1 - \frac{1}{\dot{\tau}_r} \right) \exp \left(-\frac{\dot{\tau}_r(t - t_1)}{a\sigma} \right) + \frac{1}{\dot{\tau}_r} \quad t > t_1 \quad (7)$$

The seismicity rate can now be calculated simply from (1).

$$\frac{R(t)}{r} = \begin{cases} \left[\left(1 - \frac{\dot{\tau}_r}{\dot{\tau}} \right) \exp \left(-\frac{\dot{\tau}(t-t_0)}{a\sigma} \right) + \frac{\dot{\tau}_r}{\dot{\tau}} \right]^{-1} & t_0 < t < t_1 \\ \left\{ C \exp \left(-\frac{(t-t_1)}{t_a} \right) + 1 \right\}^{-1} & t > t_1 \end{cases} \quad (8)$$

Note that if the duration of the slip event is long compared to $a\sigma/\dot{\tau}$ the seismicity rate approaches a steady state that is a factor of $\dot{\tau}/\dot{\tau}_r$ over the background rate. Following the event, as $t \rightarrow \infty$, the seismicity rate returns to background. Also note that as $\dot{\tau} \rightarrow \infty$ and $(t_1 - t_0) \rightarrow 0$ such that the product $\dot{\tau}(t_1 - t_0) \rightarrow \Delta\tau$, (8) reduces to Dieterich [1994] equation (12) which gives the Omori-like decay of events following a step change in stress.

In order to estimate the aftershock duration t_a we fit the cumulative number of earthquakes following a high frequency mainshock. Dieterich [1994] found that the number of earthquakes following a step change in shear stress $\Delta\tau$ is given by

$$N(t) = rt_a \ln \left\{ e^{\Delta\tau/a\sigma} (e^{t/t_a} - 1) + 1 \right\} \quad (9)$$

Relative Earthquake Locations.

The data are arrival times for the 2005 events determined by the Hawaiian Volcano Observatory and arrival times for the 1999-2000 events provided by the University of Wisconsin. We used a 1-D layered velocity model that approximates the 3-D model of Hansen et al.¹⁷. The 1999-2000 events were fixed at the locations determined by Hansen et al.¹⁷. To minimize potential bias from the 1-D model, we weighted the differential times between the 1999/2000 and 2005 events 3 times more heavily than the remaining differential times.